Available online at www.sciencedirect.com
SCIENCE DIRECT®
Materials Chemistry and Physics 82 (2003) 826–830
MATERIALS CHEMISTRY AND PHYSICS
www.elsevier.com/locate/matchemphys

# Electrical and dielectric properties of low-temperature crystallized $Sr_{0.8}Bi_{2.6}Ta_2O_{9+x}$ thin films on $Ir/SiO_2/Si$ substrates

Hsiu-Yu Chou [a,b], Teng-Ming Chen [a], Tseung-Yuen Tseng [c,*]

[a] Department of Applied Chemistry, National Chiao Tung University, Hsinchu 30050, Taiwan, ROC
[b] Department of Chemical Engineering, Ta Hwa Institute of Technology, Hsinchu 30037, Taiwan, ROC
[c] Department of Electronics Engineering and Institute of Electronics, National Chiao Tung University, Hsinchu 30050, Taiwan, ROC

Received 4 April 2003; received in revised form 11 July 2003; accepted 17 July 2003

**Abstract**

Ferroelectric thin films of bismuth layer structured compounds, $Sr_{0.8}Bi_{2.6}Ta_2O_{9+x}$ (SBT) were deposited onto $Ir/SiO_2/Si$ substrates using metal organic decomposition (MOD) method. The crystallization of the SBT thin films annealed at various temperatures was characterized by X-ray diffraction (XRD), scanning electron microscopy (SEM), and atomic force microscopy (AFM). The polarization (*P*) versus electric field (*E*) characteristics exhibited a systematic variation from linear to non-linear polarization (hysteresis) with an increase in the annealing temperature of the SBT films. The leakage current density and dielectric constant of the SBT films were also strongly dependent on the annealing temperature, which in turn determined the grain size, mean surface roughness and inter diffusion through interfacial layers. The lowest leakage current density of $10^{-9}$ A cm$^{-2}$ at 100 kV cm$^{-1}$ was obtained for SBT thin film annealed at 450 °C. The SBT thin films annealed at 650 and 700 °C remained fatigue-free up to $10^{11}$ switching cycles.
© 2003 Elsevier B.V. All rights reserved.

*Keywords:* Thin films; Sol–gel growth; Electrical characterization; Ferroelectricity

## 1. Introduction

Recently, the SBT ferroelectric materials have attracted the attention for the development of non-volatile random access memories (NVRAMs). Their fatigue-free polarization, endurance and high switching speed make them suitable for the fabrication of memory devices. Ferroelectric memories have been evaluated for use in two different types of memories. One is a 1T1C (1 transistor and 1 capacitor) type and another is a ferroelectric memory field-effect transistor (FeMFET). The FET type of memory has the potential for the development of non-destructive read out (NDRO) and high density non-volatile memories. The FeMFET includes the metal–ferroelectric–insulator–semiconductor (MFIS) and metal–ferroelectric–metal–insulator–semiconductor (MFMIS) structures. The ferroelectric material is placed on the gate of the transistor in these structures. It was reported that a reduction in saturation polarization and dielectric constant and an enhancement in remanent polarization/saturation polarization ratio of ferroelectric material can improve the performance of FeMFET [1–3]. Therefore, to adopt the ferroelectric materials with good properties seems to be an effective way to achieve high performance FeMFET. In the present study, we report the effect of annealing temperature on the microstructure, dielectric constant and electrical properties of metal organic decomposition (MOD) derived SBT films. Correlating the grain size to the ferroelectric and electrical properties of SBT films was also obtained.

## 2. Experiment

The SBT film with a composition of $Sr_{0.8}Bi_{2.6}Ta_2O_{9+x}$ (SBT) was prepared on $Ir/SiO_2/Si$ substrate by a method using an alkoxide–carboxylate precursor solution. Bismuth acetate [$Bi(CH_3COO)_3$], strontium acetate [$Sr(CH_3COO)_2$], and tantalum ethoxide [$Ta(CH_3COO)_5$] were selected as starting materials, and acetic acid and ethylene glycol were selected as solvent. Bismuth acetate and strontium acetate were initially dissolved in acetic acid with 30% excess bismuth at 120 °C. Then tantalum ethoxide was added to the solution to form a clear and stable precursor solution at 70 °C. The precursor solution was spin-coated on substrates. The coated thin film was dried at 150 °C for 10 min, and then 450 °C for 30 min in conventional furnace. This step

* Corresponding author.
*E-mail address:* tseng@cc.nctu.edu.tw (T.-Y. Tseng).

0254-0584/$ – see front matter © 2003 Elsevier B.V. All rights reserved.
doi:10.1016/j.matchemphys.2003.07.009

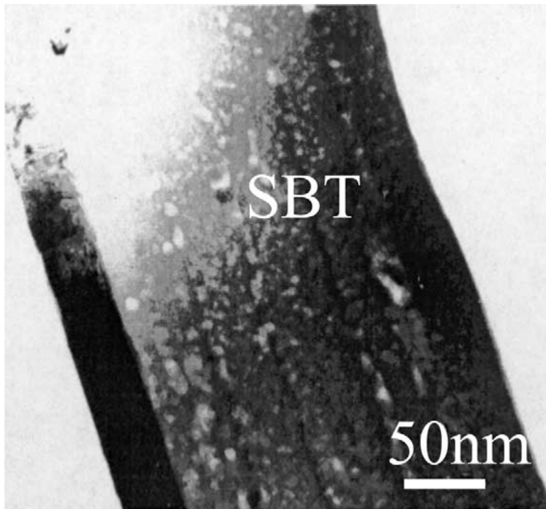


Fig. 1. TEM cross section micrograph of SBT thin film annealed at 450 °C.

was repeated several times after the desired thickness was obtained. The films were crystallized at temperatures that varied from 450 to 700 °C in oxygen atmosphere for 30 min. The thickness of SBT films is about 250 nm, which was obtained on the basis of transmission electron microscopy (TEM) and scanning electron microscope observations (as shown in Figs. 1 and 2, respectively). Pt top electrodes were deposited on the films by sputtering through a shadow mask of an area of $9.6 \times 10^{-4}$ cm$^2$.

The ferroelectric properties of SBT films were measured by RT-66A (Radiant Technologies) test system. Ferroelectric hysteresis measurements were conducted on SBT films in MFM (metal–ferroelectric–metal capacitor) configuration with a Sawyer–Tower circuit at a frequency of 500 Hz. The capacitance was measured at 100 kHz without bias voltage with a HP 4284A impedance analyzer, which can be used for obtaining dielectric constant of the films. The leakage current characteristics were measured using a HP 4146C semiconductor parameter analyzer. The surface roughnesses of the thin films annealed at various temperatures were measured using atomic force microscope (AFM). The XRD patterns were recorded using a Hitachi X-ray diffractometer with Cu Kα radiation operating at two different power levels 30 kV, 20 mA and 50 kV, 200 mA in order to investigate the crystallinity and the phases of the SBT thin films. The grain sizes were calculated from the full width at half maximum (FWHM) of the (1 1 5) diffraction peak using Scherrer's equation. The chemical composition of the films was determined using inductively coupled plasma (ICP) mass spectroscopy (Perkin Elmer, SCIEX ELAN 5000) and secondary ion mass spectroscopy (SIMS, CAMECA IMS-4f).

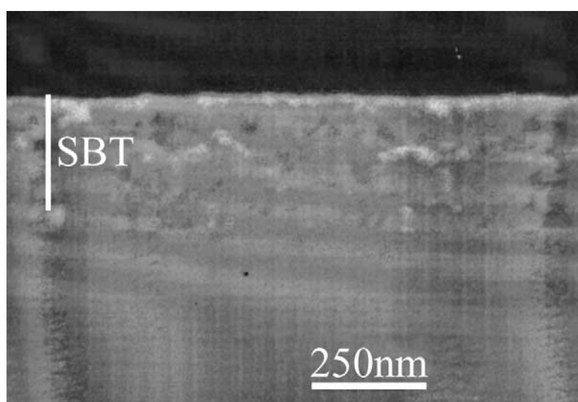


Fig. 2. SEM cross section micrographs of SBT thin film annealed at 550 °C.

## 3. Results and discussion

Fig. 3(a) shows the XRD patterns, which indicate SBT single phase for the SBT thin films annealed at various temperatures. The 450 °C annealed film has poor crystallinity while 700 °C annealed film is well crystallized. The XRD pattern shows a broadened line corresponding to (1 1 5) peak when a high power radiation (50 kV and 200 mA) is impinged on the films (Fig. 3(b)). The line broadening may arise due to two possible reasons. One reason may be the shift in lattice constants when the film is composed of crystalline grains of different sizes. Another possible reason could be the small

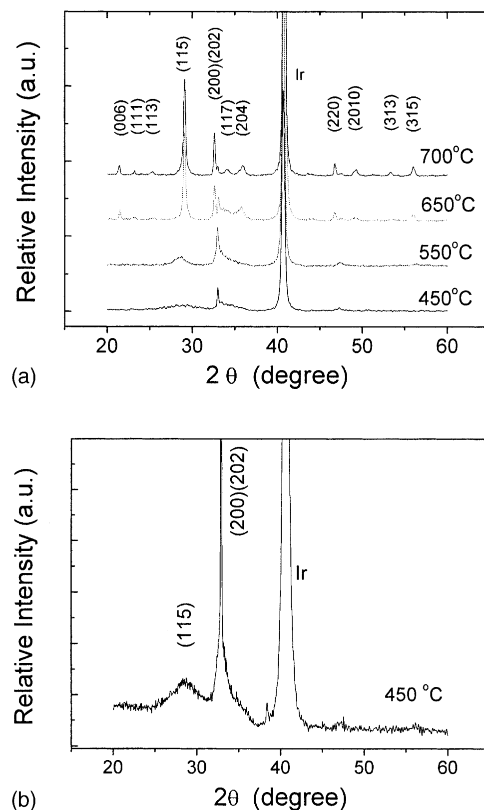


Fig. 3. XRD pattern of SBT thin films (a) annealed at various temperatures indicated with 30 kV, 20 mA radiation and (b) annealed at 450 °C with 50 kV, 200 mA radiation.

Table 1
The composition and XRD grain size of SBT thin films annealed at various temperatures

| Annealing temperature (°C) | Bi/Ta | Sr/Ta | Grain size (nm) |
|---|---|---|---|
| 450 | 1.290 | 0.368 | 8.90 |
| 550 | 1.279 | 0.366 | 10.80 |
| 650 | 1.209 | 0.365 | 13.20 |
| 700 | 1.158 | 0.361 | 13.68 |

crystalline grain size of poor crystallinity of the films. In this study, the grain sizes of the films are quite uniform from SEM and TEM observations (Figs. 1 and 2), the first case scenario may be ruled out. Hence the line broadening of (1 1 5) peak in 450 and 550 °C annealed SBT thin films can be regarded as a result of small grain size. The grain size ($d_{XRD}$) was calculated from the FWHM of the (1 1 5) diffraction peak using the Scherrer's equation [4]

$$d_{XRD} = \frac{K\lambda}{\beta\cos\theta}$$

where $\lambda$ is the X-ray wavelength, $\beta$ the FWHM of the diffraction line, $\theta$ the angle of diffraction, and the constant $K = 0.9$. If $B$ and $b$ are the measured FWHM, of equivalent diffraction lines in the specimen and the reference, respectively, the FWHM of the true diffraction profile will be given by

$$\beta^2 = B^2 - b^2 \quad \text{(for a Gaussian line shape)}$$

Table 1 lists the grain sizes calculated from XRD results and compositions of SBT thin films annealed at various temperatures. The grain size increases with increasing annealing temperature up to 650 °C.

Fig. 4 depicts *P–E* hysteresis loops of SBT thin films annealed at various temperatures. It shows that the remanent polarization of the SBT films increases with increasing annealing temperature except the loop at 450 °C. The 450 °C annealed film exhibits linear *P–E* relation due to the poor crystalline SBT phase (Fig. 3(a)). Such ferroelectric behavior is obviously related to grain size of the films (Table 1). The SBT films with larger grain sizes exhibit better ferroelectric properties. The ferroelectric properties are governed by the ferroelectric domain structure, domain nucleation, and domain mobility. Ren et al. [5,6] have correlated the grain size of the ferroelectric films to the domain structure and the domain wall mobility based on the TEM observations of $PbTiO_3$ thin films. The grains having dimensions close to those of single domain have been found to be very stable under an external field, which implies the domain nucleation in such samples very difficult. Consequently, poor ferroelectric properties obtained in a single-domain-predominated film, which usually has small grains. Therefore, a small remanent polarization is expected in ferroelectric films with small grains. On the other hand, the film having large grains with multi-domain-predominated structure can be easily switched leading to large remanent polarization. That is, the ferroelectric properties were dependent on the grain size. In the present study, the observation of increase in remanent polarization with increasing grain size of SBT films is shown in Fig. 4 and Table 1, which agrees well with the phenomena of grain size dependence of ferroelectricity in thin films as reported by Ren et al. [5,6].

Fig. 5 depicts the variation of dielectric constant of SBT thin films with annealing temperature, indicating that the dielectric constant increases with increasing annealing temperature, which results in improved crystallinity and larger grain size of the SBT film. Arlt et al. [7] have pointed out that the grain size dependence of dielectric permittivity was more pronounced for $BaTiO_3$ samples with grain sizes less than 0.7 μm. Through theoretical calculation [7], they concluded that the density of 90° domain walls was inversely proportional to the square root of the grain size and thus the area of 90° domain walls contributed to the reduction of dielectric permittivity per unit volume increased with the decrease of grain size. Moreover, the pinning effect of the domain walls also contributed to the reduction in polarization [4,7]. The smaller the grain size, the more the pinning

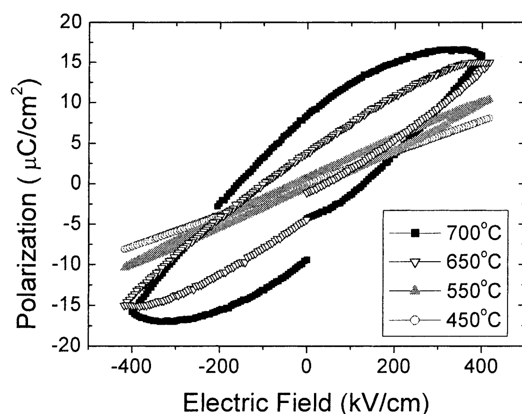


Fig. 4. *P–E* hysteresis loops of SBT thin films annealed at various temperatures.

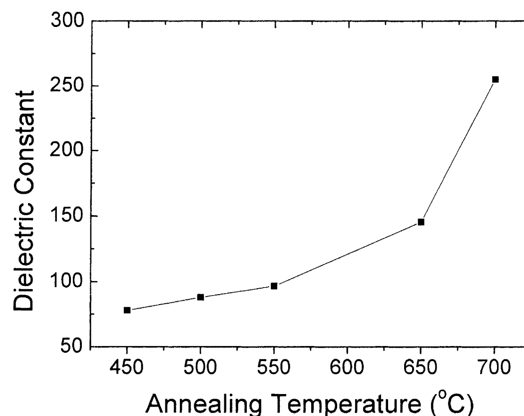


Fig. 5. Variation of dielectric constant of SBT thin films with annealing temperature.

effect, the less the domain wall mobility of SBT thin films is. The resultant reduction in the wall mobility would decrease the switching rate, thereby lowering the dielectric constant. Under the consideration of small difference in grain size between 650 and 700 °C films but having large difference in dielectric constant between them (Table 1 and Fig. 5), large leakage current for 700 °C films would be one of the main causes leading to its high dielectric constant. Dickens et al. [8] have found that the polarization was partly contributed by the leakage current. The higher polarization would lead to the higher dielectric constant, so the higher dielectric constant could contribute from the larger leakage current of the films annealed at higher temperature, such as 700 °C. Lower values of remanent polarization have also been recorded for smaller grain sizes of the SBT films as evidenced by the *P–E* hysteresis loops shown in Fig. 4.

The ICP compositional analysis indicates that Sr/Ta and Bi/Ta ratios in the annealing films are slightly less than those in the initial precursor solution (Table 1). The reason for such compositional variation is expected to be the loss of bismuth from the SBT thin films by evaporation and diffusion into the bottom electrode. This result is further confirmed by SIMS depth profile analysis as indicated in Fig. 6, which shows obviously the variation in bismuth content at the surface of SBT film and interface of SBT/Ir. The bismuth content of SBT thin films increases with increasing annealing temperature from 650 to 700 °C at near the edge of Ir bottom electrode. It is presumed that the Bi depletion might result from the oxidation of Bi at the interface [9]. The oxygen concentration increases at SBT/Ir interface as shown in Fig. 6, which may be attributed to Bi and Ir oxidized during the process. This change might promote the crystallization of SBT films and increases the film surface roughness that leads to larger leakage current density at higher annealing temperature as indicated in Fig. 7, which shows the leakage current density versus electric field for SBT films annealed at various temperatures.

The leakage current density is lower than $10^{-9}$ A cm$^{-2}$ at an applied electric field of 100 kV cm$^{-1}$ for the film annealed at 450 °C. Such film shows smaller grain size (Table 1) and smaller surface roughness relative to other thin films as shown in Fig. 8. The leakage current is increased with an increase in surface roughness of SBT thin films (Fig. 8), which is due to the fluctuation of the surface height occurred and consequently the local electric field various from place to place [10–12]. When an electric field is applied

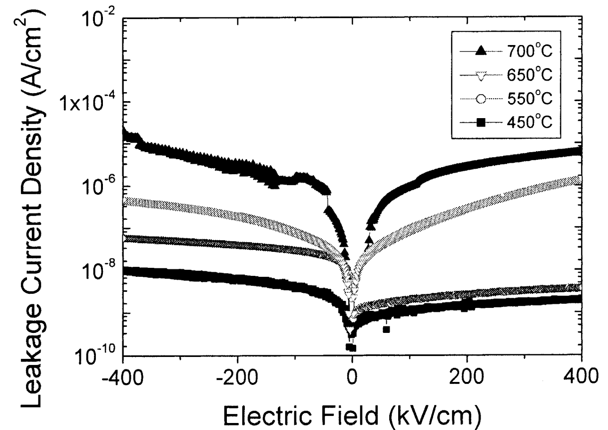


Fig. 7. Curves of leakage current density versus applied electric field for SBT thin films annealed at various temperatures indicated.

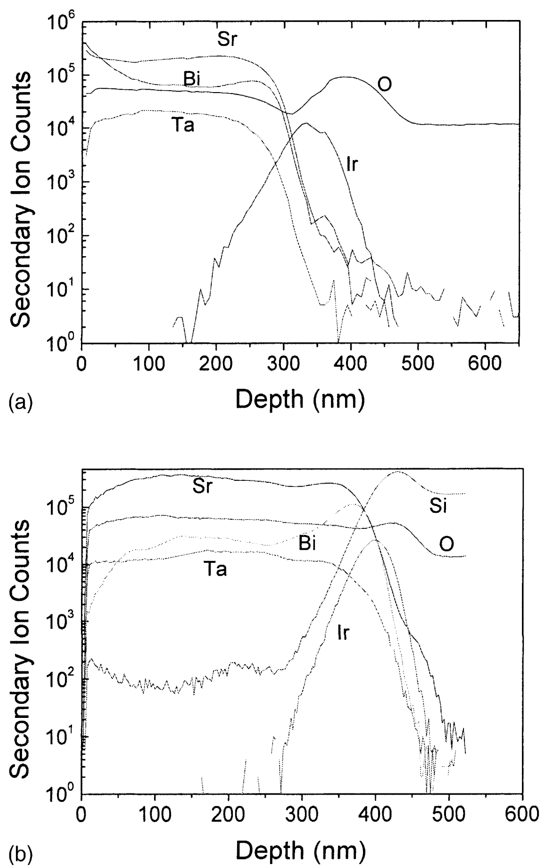


Fig. 6. SIMS depth profiles of SBT thin films annealed at: (a) 650 °C and (b) 700 °C, for 30 min.

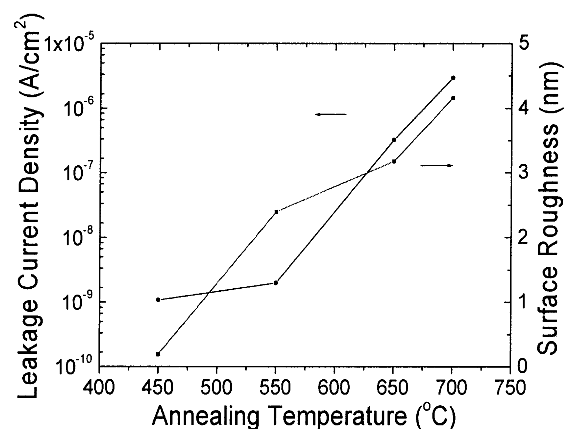


Fig. 8. Variation of surface roughness and leakage current density at 100 kV cm$^{-1}$ of SBT thin films with annealing temperature.

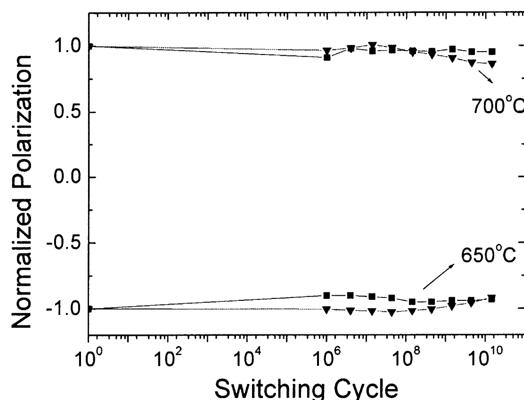


Fig. 9. Fatigue characteristics of SBT thin films annealed at 650 and 700 °C under 5 V bipolar switching cycles.

to SBT thin film capacitors with high surface roughness, the electric field concentrates in the deep valleys between SBT grains and hence a higher leakage current density is observed.

Fig. 9 shows the remanent polarization as a function of switching cycles for the films annealed at 650 and 700 °C for 30 min. Both films exhibited good fatigue-free behavior up to $10^{11}$ switching cycles. The fatigue behavior is predominantly related to oxygen vacancy formation and stability in $Bi_2O_2$ layers and Sr–Ta–O perovskite blocks [13–15]. The relative stability of Sr–Ta–O perovskite blocks of SBT thin film results in its fatigue-free behavior.

## 4. Conclusions

The SBT thin films were prepared on $Ir/SiO_2/Si$ substrate by metal organic deposition and annealed at various temperatures. The single phase SBT thin film was obtained at a low temperature of 450 °C. The dielectric constant and the polarization versus electric-field hysteresis loop of the SBT films increased with increasing annealing temperature due to the consistent increase in grain size and crystallinity. The composition analysis of SBT thin films indicated a loss at higher annealing temperatures due to the bismuth evaporation and diffusion into the bottom electrode. The leakage current density of SBT thin films decreased as annealing temperature decreased. The thin film annealed at 450 °C has a low leakage current value of $10^{-9}$ A cm$^{-2}$ at an applied field of 100 kV cm$^{-1}$, which may be due to small grain size, less surface roughness and no interface layer formation. The SBT thin films have a fatigue-free property up to $10^{11}$ switching cycles.

## References

[1] H.T. Lue, C.J. Wu, T.Y. Tseng, IEEE Trans. Electron Dev. 49 (2002) 1790.
[2] H.T. Lue, C.J. Wu, T.Y. Tseng, IEEE Trans. UFFC 50 (2003) 5.
[3] T.Y. Tseng, S.Y. Lee, Appl. Phys. Lett. 83 (2003) 981.
[4] S. Chattopadhyay, P. Ayyub, V.R. Palkar, M. Multani, Phys. Rev. B 52 (1995) 13177.
[5] S.B. Ren, C.J. Lu, J.S. Liu, H.M. Shen, Y.N. Wang, Phys. Rev. B 54 (1996) R14337.
[6] S.B. Ren, C.J. Lu, J.S. Liu, H.M. Shen, Y.N. Wang, Phys. Rev. B 55 (1997) 3485.
[7] G. Arlt, D. Henngings, G. de With, J. Appl. Phys. 58 (1985) 1619.
[8] B. Dickens, E. Balizer, A.S. DeReggi, S.C. Roth, J. Appl. Phys. 72 (1992) 4258.
[9] B.K. Moon, C. Isobe, K. Hironaka, S. Hishikawa, J. Appl. Phys. 89 (2001) 6557.
[10] Y.P. Zhao, G.C. Wang, T.M. Lu, G. Palasamtzas, J.Th.M. De Hosson, Phys. Rev. B 60 (1999) 9157.
[11] Y.S. Kim, M.Y. Sung, Y.H. Lee, B.K. Ju, M.H. Oh, J. Electrochem. Soc. 146 (1999) 3398.
[12] Y.S. Kim, Y.H. Lee, K.M. Lin, M.Y. Sung, Appl. Phys. Lett. 74 (1999) 2800.
[13] S.E. Cummins, J. Appl. Phys. 35 (1964) 3045.
[14] B.H. Park, S.J. Hyun, S.D. Bu, T.W. Noh, J. Lee, H.D. Kim, T.H. Kim, W. Jo, Appl. Phys. Lett. 74 (1999) 1907.
[15] B.H. Pak, B.S. Kang, S.D. Bu, T.W. Noh, J. Lee, W. Jo, Nature 401 (1999) 682.